
Graph Backup: Data Efficient Backup Exploiting Markovian Transitions

Zhengyao Jiang

University College London

zhengyao.jiang.19@ucl.ac.uk

Tianjun Zhang

University of California, Berkeley

tianjunz@berkeley.edu

Robert Kirk

University College London

robert.kirk.20@ucl.ac.uk

Tim Rocktäschel

University College London

tim.rocktaschel@ucl.ac.uk

Edward Grefenstette

University College London

e.grefenstette@ucl.ac.uk

Abstract

The successes of deep Reinforcement Learning (RL) are limited to settings where we have a large stream of online experiences, but applying RL in the data-efficient setting with limited access to online interactions is still challenging. A key to data-efficient RL is good value estimation, but current methods in this space fail to fully utilise the structure of the trajectory data gathered from the environment. In this paper, we treat the transition data of the MDP as a graph, and define a novel backup operator, Graph Backup, which exploits this graph structure for better value estimation. Compared to multi-step backup methods such as n -step Q -Learning and $\text{TD}(\lambda)$, Graph Backup can perform counterfactual credit assignment and gives stable value estimates for a state regardless of which trajectory the state is sampled from. Our method, when combined with popular value-based methods, provides improved performance over one-step and multi-step methods on a suite of data-efficient RL benchmarks including MiniGrid, Minatar and Atari100K. We further analyse the reasons for this performance boost through a novel visualisation of the transition graphs of Atari games.

1 Introduction

Deep Reinforcement Learning (DRL) methods have achieved super-human performance in a varied range of games (Mnih et al., 2015; Silver et al., 2016; Berner et al., 2019; Vinyals et al., 2019). All of these present a proof of existence for DRL: with large amount of online interaction, DRL-trained policies can learn to solve problems that have similar properties to real-world decision making tasks. However, most real-world tasks such as autonomous driving or financial trading are hard to simulate, and generating new interaction data can be expensive. This makes it crucial to develop data-efficient RL approaches that solve sequential decision-making problems with limited environment interactions.

As many existing DRL algorithms assume access to a simulator they don't focus on efficiently using the available data as it's always cheaper to simply generate fresh data from the simulator. Data is normally stored in a buffer and only used several times for learning before being discarded. This means these algorithms underutilise the data that is generated from the simulator, ignoring potential gains in learning through exploiting additional structure in this data. However, there is lots

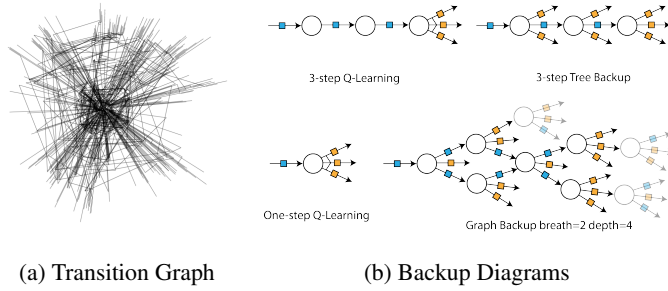


Figure 1: (a) shows the transition graph Frostbite, an Atari game. (b) shows backup diagrams for different backup targets. The blue squares represent the state-action pairs that have been observed, orange squares are actions where target net evaluation happened, and circles are states

of additional structure, and a key insight of our work is to organise the trajectories stored in the buffer as a graph (For example see Figure 1(a) which shows a visualisation of the transition graph of the Atari game Frostbite). Our method, Graph Backup, then exploits this transition graph to provide a novel backup operator for bootstrapped value estimation. When estimating the value of a state, it will combine information from a subgraph rooted at the target state, including rewards and value estimates for future states.

When the environment has Markovian transitions and crossovers between trajectories, the construction of this data graph provides several benefits. As discussed in Section 4.2, our method exploits intersecting trajectories to correctly propagate reward to more states, effectively by propagating reward along an imagined trajectory. Further, while existing improvements to one-step backup (as used in by Mnih et al. (2015)) such as multi-step backup (Moriarty and Miikkulainen, 1995; Hessel et al., 2018; Sutton and Barto, 2018) address the problem of slow reward information propagation (Hernandez-Garcia and Sutton, 2019), they add variance to the state value estimates as different states can have different values estimates depending on the trajectory they were sampled from (Figure 2). Our method addresses this issue through grouping states in the transition graph and averaging over outgoing transitions at the value estimation stage.

We propose a specific implementation of Graph Backup, extending Tree Backup (Precup et al., 2000) (Section 4, see Figure 1(b)). Our method improves data efficiency and final performance on MiniGrid (Chevalier-Boisvert et al., 2018), Minatar (Young and Tian, 2019) and Atari100K when using Graph Backup combined with DQN (Mnih et al., 2015) and Data-Efficient Rainbow (van Hasselt et al., 2019) compared to other backup methods, showing that utilising the graph structure of the trajectory data leads to improved performance in the data-efficient setting (Section 5). To more fully understand where this gain in performance comes from, we further investigate the graph sparsity of different environments in relation to the performance of Graph Backup, in part using a novel method to visualise the full set of seen transitions and their graph structure (Section 6).

2 Related Work

The idea of multi-step backup algorithms (e.g. TD(λ), n -step TD) dates back to early work in tabular reinforcement learning (Sutton, 1988; Sutton and Barto, 2018). Two approaches to multi-step targets are n -step methods and eligibility trace methods. The n -step method is a natural extension of using a one-step target that takes the rewards and value estimations of n steps into future into consideration. For example, the n -step SARSA (Rummery and Niranjan, 1994; Sutton and Barto, 2018) target for step t is simply the sum of n -step rewards and the value at timestep $t + n$: $R_{t+1} + R_{t+2} + \dots + R_{t+n-1} + V(S_{t+n})$. Graph Backup is an extension of an n -step backup target, Tree Backup, which will be described in Section 3.

Eligibility trace (Sutton, 1988) methods instead estimate the λ -return, which is an infinite weighted sum of n -step returns. The advantage of the eligibility trace method is it can be computed in an online manner without explicit storage of all the past experiences, while still computing accurate target value estimates. However, in the context of off-policy RL, eligibility traces are not widely applied because the use of a replay buffer means all past experiences are already stored. In addition,

eligibility traces are designed for the case with a linear function approximator, and it's nontrivial to apply them to neural networks. van Hasselt et al. (2021) proposed an extension of the eligibility trace method called *expected eligibility traces*. Similar to Graph Backup, this allows information propagation across different episodes and thus enables counterfactual credit assignment. However, similar to the original eligibility traces methods, it is a better fit for the linear and on-policy case, whereas Graph Backup is designed for the non-linear and off-policy cases.

Since a learned model can be treated as a distilled replay buffer (van Hasselt et al., 2019), we can view model-based reinforcement learning as related to our work. Recent examples include Schriftwieser et al. (2020); Hessel et al. (2021); Farquhar et al. (2018); Hafner et al. (2021a); Kaiser et al. (2020a); Ha and Schmidhuber (2018). These MCTS-based algorithms also share some similarities with Graph Backup as they are also utilise tree-structured search algorithms. However, our work is aimed at model-free RL, and so is separate from these works.

Several recent works have also utilised the graph structure of MDP transition data. Zhu et al. (2020) propose the using the MDP graph as an associative memory to improve Episodic Reinforcement Learning (ERL) methods. This allows counterfactual reward propagation and can improve data efficiency. However, the usage of a data graph in this work is different from the usage in Graph Backup: the graph is used for control and as an auxiliary loss, rather than for target value estimation. Their associative memory graph also doesn't handle stochastic transitions and the return for each trajectory is only based on observed return (no bootstrapping is used), unlike our work. Topological Experience Replay (Anonymous, 2022, TER) uses the graph structure of the data in RL for better replay buffer sampling. TER uses the graph structure to decide which states should be sampled from the replay buffer during learning, by implementing a sampling mechanism that samples transitions closer to the goal first. This work is orthogonal (and possibly complementary) to ours, as TER is a replacement for uniform or prioritized sampling from a replay buffer while Graph Backup is a replacement for one-step or multistep backup for value estimation.

3 Preliminaries: One-step and Multi-step Backup

Given an MDP \mathcal{M} we denote \mathcal{A} as the action space; \mathcal{S} to be state space; $\mathcal{R} \subset \mathbb{R}$ to be reward space; and $a_t \in \mathcal{A}$, $s_t \in \mathcal{S}$ are used to denote the specific actions and states respectively observed at step t . We denote a trajectory of states, actions and rewards as $\tau = (s_1, a_1, r_1, s_2, a_2, r_2, \dots)$.

For a transition (s_t, a_t, r_t, s_{t+1}) the loss function of DQN methods is defined as the mean square error¹ between the predicted q -value and the backup target G^{a_T} for (s_t, a_t) :

$$L(\theta|s_t, a_t) \stackrel{\text{def}}{=} (q_\theta(s_t, a_t) - G^{a_t})^2, \quad (1)$$

where q_θ represents the online network parameterized by θ . The backup target G^{a_T} is an estimation of the optimal Q-value $q^*(s_t, a_t)$. Vanilla DQN uses one-step bootstrapped backup, which makes gradient descent an analog to the update of tabular Q -learning:

$$G_{t:t+1}^{A_t} \stackrel{\text{def}}{=} r_{t+1} + \gamma \max_{a'} q_{\theta'}(s_{t+1}, a'). \quad (2)$$

The one-step target makes the propagation of the reward information to previous states slow, which is amplified by the use of a separate frozen target network. This motivates the use of more sample efficient multi-step targets in DQN (Hessel et al., 2018; Hernandez-Garcia and Sutton, 2019).

A widely used multi-step backup algorithm is n -step Q -Learning (n -step- Q) (Hessel et al., 2018; Silver et al., 2017). This method sums the rewards in next n steps, together with the maximum q value at step n :

$$G_{t:t+n}^a \stackrel{\text{def}}{=} r_{t+1} + \gamma r_{t+2} + \dots + \gamma^n \max_{a'} q_{\theta'}(s_{t+n}, a'). \quad (3)$$

n -step- Q exploits the chain structure of the trajectories with little computational cost, but at a cost of biased target estimation. The distribution of the sum of the rewards $r_{t+1} + \gamma r_{t+2} + \dots + \gamma^{n-1} r_{t+n}$ are conditioned on the behaviour policy μ which generates the data. This means that in a off-policy setting the estimated target value can be biased towards the value of the behaviour policy.

¹Or sometimes the Huber Loss (Huber, 1992)

Another off-policy multi-step target is Tree Backup (Precup et al., 2000). Tree Backup is designed for general purpose off-policy evaluation, meaning it aims to estimate the value of any target policy π by observing the behaviour policy μ . When the target policy is the optimal policy given by $q_{\theta'}$, Tree Backup recursively applies one-step- Q backup to the trajectory, bootstrapping with the target value network when the input action a isn't that taken in the trajectory (a_t):

$$G_{t:t+n}^a \stackrel{\text{def}}{=} \begin{cases} r_{t+1} + \gamma \max_{a'} G_{t+1:t+n}^{a'}, & \text{if } t < n, a = a_t \\ q_{\theta'}(s_t, a), & \text{otherwise.} \end{cases} \quad (4)$$

Despite what it's name suggests, Tree Backup does not expand a tree of states and transitions, and so still only leverages the chain structure of trajectories. The name is because the trajectory has leaves corresponding to the actions that were not selected in the current trajectory. In Figure 1(b) we show the backup diagram of the 3-step Tree Backup, where yellow squares are these leaf actions.

4 Graph Backup

In this section we introduce a new graph-structured backup operator, Graph Backup, extending the multi-step method Tree Backup. Graph Backup allows counterfactual reward propagation and variance reduction while also having the benefits of multi-step backup.

4.1 Introducing Graph Backup

We propose the Graph Backup operator that propagates temporal differences across the whole data graph rather than a single trajectory. The differences between one-step, multi-step, tree and Graph backup are illustrated in Figure 1(b).

We want a backup method that can work with stochastic transitions, which means a single state-action pair can lead to different states. This means it's not obvious how to perform recursive backups to the next state, as there could be multiple next states. We estimate the transition probability to each next state using visitation counts, and to use the estimated transition probabilities to compute the empirical mean over all possible state value estimates weighted by the likelihood of transitioning to that state. This is easy to calculate efficiently and provides strong results as seen in Section 5.

Denoting the set of all seen transitions to be $\mathcal{T} \subseteq \mathcal{S} \times \mathcal{A} \times \mathcal{R} \times \mathcal{S}$, a counter function $f : \mathcal{T} \rightarrow \mathbb{N}^+$ maps each transition $T = (s, a, r, s')$ to its frequency $f(T)$. The Graph Backup target for a state-action pair (s, a) is then the average of recursive one-step backup of all outgoing transitions. Similar to Tree Backup, if the (s, a) has not been seen, the target is estimated directly by the target network.

Define $\mathcal{T}_{s,a} \stackrel{\text{def}}{=} \{(\hat{s}, \hat{a}, \hat{r}, \hat{s}') \in \mathcal{T} | \hat{s} = s, \hat{a} = a\}$, the set of all $(\hat{s}, \hat{a}, \hat{r}, \hat{s})$ tuples starting with s, a . Extending Tree Backup, we can then define the *Graph Backup* (GB) value estimate as

$$G_s^a \stackrel{\text{def}}{=} \begin{cases} \frac{1}{c(s,a)} \sum_{T \in \mathcal{T}_{s,a}} f(T) \left(\hat{r} + \gamma \sum_{a'} \pi(a'|\hat{s}') G_{\hat{s}'}^{a'} \right) & \text{if } c(s,a) > 0 \\ q_{\theta'}(s, a) \text{ otherwise.} \end{cases} \quad (5)$$

where $c(s, a) = \sum_{T \in \mathcal{T}_{s,a}} f(T)$ is the normaliser, π is the target policy and $q_{\theta'}$ is the target network. In the case where target policy always chooses the action with optimal Q value $\pi(a|s) = \mathbb{1}(\text{argmax}_{a'} G_s^{a'} = a)$, the formula can be simplified into:

$$G_s^a \stackrel{\text{def}}{=} \begin{cases} \frac{1}{c(s,a)} \sum_{T \in \mathcal{T}_{s,a}} f(T) \left(\hat{r} + \gamma \max_{a'} G_{\hat{s}'}^{a'} \right) & \text{if } c(s,a) > 0 \\ q_{\theta'}(s, a) \text{ otherwise.} \end{cases} \quad (6)$$

This is often the case since our implementations are based on DQN and we are interested in the optimal Q-value. In this paper *Graph Backup* refers to the simplified version in Equation (6).

Our Graph Backup implementation extends Tree Backup. However, there could be other implementations which extend other multi-step method, such as n -step- Q backup or the n -step version (Hernandez-Garcia and Sutton, 2019) of Retrace (Munos et al., 2016). In Appendix J, we present a variation of Graph Backup that extends n -step- Q backup.

Note that in Equations (6), (7) and (8), the graph structure does not appear explicitly. This is because it's easier to mathematically formalise these backup operators using transition counts; from an

implementation perspective building and maintaining the data graph is the most efficient way of calculating these target value estimates. To better provide intuition for Graph Backup, in Appendix D we explicitly describe the data graph generated from an MDP and link that to Equation (6). The data graph contains the information for calculating and sampling from \mathcal{T} , \mathcal{T}_s , $\mathcal{T}_{s,a}$, $c(s, a)$, $c(s)$ and $f(\mathcal{T})$.

4.2 Advantages of Graph Backup

In Figure 2 we show how Graph Backup brings benefits to value estimation and thus the learning of the agent. Assuming the value estimation of all the states are initialised as 0, the one-step backup can update the value of only 1 state. The multi-step backup methods can further propagate the reward to the whole trajectory that leads to the reaching of the goal.² However, Graph Backup goes beyond that and propagates rewards to the states of another trajectory (the dashed line). This feature of counterfactual reward propagation can significantly benefit the credit assignment of sparse reward tasks: During the exploration of a sparse-reward environment, policies usually generate a large number of trajectories that do not reach the goal, and while multi-step methods cannot efficiently leverage those transitions, Graph Backup can reuse them by propagating rewards from the crossovers with other successful trajectories.

The second row of Figure 2 shows another advantage of Graph Backup: reducing the variance of the value estimate. Multi-step backup in this case will assign different value estimations for the same state depending on the trajectory the state is sampled from (as it will appear multiple times in the replay buffer). This brings extra noise to the value estimate that can be harmful to learning. In the Figure 2, the noise comes from different rewards in different trajectories. When combined with function approximation and SGD, such noise can also be generated by generalisation error and the stochastic optimization process. In Section 6, we showed a simple case in MiniGrid where this target value noise can constantly disturb the convergence of DQN. On the other hand, Graph Backup effectively avoids the extra variance by averaging the trajectories branching from the same state-action pair. If we consider the case of value estimation of an arbitrary policy (e.g. in Equation (5)), Graph Backup also reduces the variance caused by the stochastic policy.

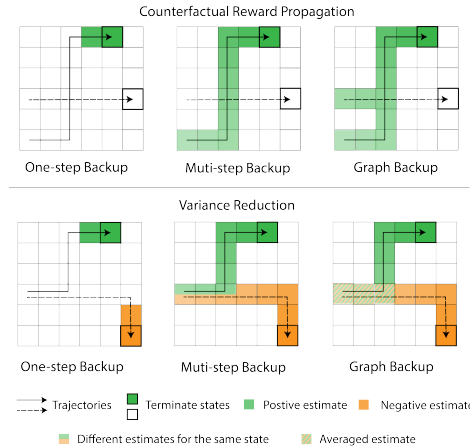


Figure 2: Benefits of Graph Backup

4.3 Limiting Expansion of the Graph

A naïve implementation of Graph Backup would follow the definition exactly and do an exhaustive recursive expansion of the graph. However, the computational cost of doing so can quickly blow up with the size of the replay data.³ Therefore, similar to the n -step backup methods, we need to limit recursive calls. For Graph Backup, this means expanding a smaller local graph from the source state, using the target network for value estimation when reaching expansion limits. In our work, the

²In this case, both Tree Backup and n -step- Q backup can produce the estimation shown in the example tasks.

³In fact, if there are loops in the graph, the situation can be even worse as the algorithm may never converge.

expansion of the local data graph has both a breadth limit b and a depth limit d . When the breadth limit is hit ($|\mathcal{T}_{s,a}| > b$), we will sample b transitions from $\mathcal{T}_{s,a}$ according to their frequency f , as opposed to expanding all transitions. If the depth limit is hit ($d < n$) the expansion of the graph will be terminated (so the second case in Equations (6) and (7) is taken).

The pseudocode for local graph expansion is shown in Algorithm 1. Figure 1(b) also illustrates examples of limited expansion for Graph Backup, where faded nodes are clipped away due to hitting the limit. Notably, in our implementation the breadth limit a is bound on the number of transitions, not the number of states. This is relevant when two actions lead to the same next state, which would count as two transitions rather than one.

In general, the exact approach to expanding the local graph can inject inductive biases that will affect the data efficiency and the computational costs. In our work, we make sure the expansion will reach d steps in order to better align with multi-step methods. This makes sure the algorithm will reduce to Tree Backup gracefully when there are no crossovers between the trajectories. It also allows a more principled comparison between Tree Backup and Graph Backup. For $b = 1$ Graph Backup will do a d -step Tree Backup with trajectories sampled from the transition graph rather than real trajectories, and increasing b will gradually make the Graph Backup leverage more structure from the transition graph.

4.4 Integration of Other Rainbow Components

To demonstrate that Graph Backup improves data efficiency in a realistic state-of-the-art algorithm, we integrate Graph Backup inside Rainbow (Hessel et al., 2018). As a replacement for n -step- Q backup, Graph Backup is orthogonal to all other ingredients. While some components such as prioritized experience replay(PER) (Schaul et al., 2016), noisy networks (Fortunato et al., 2018) and duelling network architectures (Wang et al., 2016) can be plugged in seamlessly, others require more care, which we describe here.

Combining double DQN (van Hasselt et al., 2016) with Tree Backup and Graph Backup is quite straightforward. Double DQN uses an online network instead of target network to specify the optimal policy in the bellman update, so that $\max_a q_{\theta'}(s, a) = q_{\theta'}(s, \arg\max_a q_{\theta'}(s, a))$ becomes $q_{\theta'}(s, \arg\max_a q_{\theta}(s, a))$ in one-step or n -Step-Q backup. For Tree Backup and Graph Backup, we can take the same approach for every expanded state.

Distributional RL (Bellemare et al., 2017), specifically C51, attempts to model the whole distribution of the state-action value rather than the expectation, using a distributional version of the bellman update (namely, one-step backup) when applied in the DQN setting. C51 divides the support of the value into discrete bins, called atoms, and the q network then outputs categorical probabilities over the atoms. In the distributional bellman update, the vanilla bellman update is applied to each atom, and the probability of the atom is distributed to the immediate neighbours of the target value. The loss is the KL divergence between target and predicted value distribution rather than mean squared error. In order to combine C51 and Tree Backup or Graph Backup, we apply the distributional bellman update in every state node.

In Algorithm 2, we combine double and distributional RL with Graph Backup given the subgraph state list calculated by Algorithm 1. Blue lines show the changes introduced by Graph Backup.

4.5 Assumptions

The effectiveness of Graph Backup relies on two assumptions about the environment: (1) the transition function of the environment is Markovian, and (2) there are crossovers between state trajectories. We show in Section 5 that—perhaps counter-intuitively—these assumptions hold frequently enough in high dimensional environments (Atari100 from pixel input) for Graph Backup to differentiate itself from Tree Backup in a statistically significant manner. As such, these restrictions are not as strict as may appear, and we further discuss how they can be relaxed in Section 7.1.

5 Experiments

In order to test whether Graph Backup can bring benefits to the data efficiency of a DRL agent, we conduct experiments on singleton-MiniGrid, MinAtar and Atari100K. These tasks have an

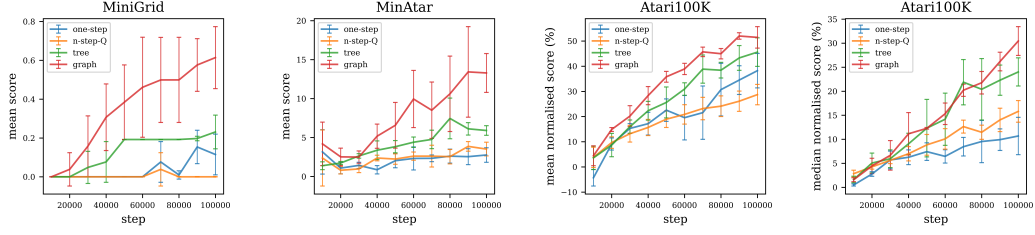


Figure 3: Summary of training curve for Minigrid, Minatar and Atari100K. Each curve is the average/median of all the tasks within a task group. For Atari A100K, we show both the mean and median of the human-normalised scores.

increasingly sparse transition graph so that we can see how many crossovers are needed for Graph Backup to bring significant performance improvements. The baseline agent for MiniGrid and MinAtar is DQN (Mnih et al., 2015) and for Atari100K is Data-Efficient Rainbow (van Hasselt et al., 2019). The average training curves of the different backup methods are shown in Figure 3, where we run each algorithm for 5 random seeds. The performance metric for Atari in the plot is the mean and median of human-normalised scores (%). The final performance for each task and method can be found in Table 1, where we also include both mean and median metrics. The full results of each individual tasks are shown in Table 2 in Appendix.

MiniGrid We first compare the methods in 5 singleton MiniGrid tasks: Empty8x8, DoorKey6x6, KeyCorridorS3R1, SimpleCrossingS9N2 and LavaCrossingS9N2. Every single run (out of 5) has a different but fixed random seed within the whole training process. We set the environment to be fully observable so that the transitions are Markovian. The overall number of possible states is small and the data graph is thus quite dense. The reward of MiniGrid is only

given at the end of the episode, which makes credit assignment a critical problem. Among the 5 tasks, one-step backup and Tree Backup only managed to converge within $1e5$ steps for the easiest empty room task. For other tasks with more complex navigation (SimpleCrossing and LavaCrossing) and interaction with objects (DoorKey and KeyCorridor), only the Graph Backup converged this low data regime.

Minatar We perform experiments on Minatar. Minatar is a collection of miniature Atari games with a symbolic representation of the objects. The game state is fully specified by the observation of a 10 by 10 image, where each pixel corresponds to an object. We set the overall number of interactions to be 100,000, inspired by the Atari100K benchmark (Kaiser et al., 2020a). We can see in Figure 3 that Graph Backup outperforms Tree Backup, n -step- Q backup and one-step backup in terms of mean scores. Looking at individual tasks, we find out that most of the improvements of Graph Backup comes from a single task, Freeway, which is a sparse reward task. This, together with the results of MiniGrid, shows that the power of Graph Backup plays an important role in sparse reward problems, potentially because of the counterfactual reward propagation.

Atari100K In order to test if Graph Backup can be applied on tasks with pixel observations, we test it in Atari100K. As suggested by its name, Atari100K limits the number of interactions of Atari games to be 100,000, which is equivalent to 2 hours of game-play in Atari. Since the human performance scores reported by Mnih et al. (2015) are also from human experts after 2 hours of game-play, Atari100K is considered as a test-bed for human-level data-efficient learning. We follow the standard frame processing protocol used by Rainbow Hessel et al. (2018) without any other

Table 1: Numeric summary of the performance

	one-step	n -step- Q	tree	graph
MiniGrid-mean	0.14	0.02	0.2	0.58
MiniGrid-median	0.0	0.0	0.0	0.58
MinAtar-mean	3.07	3.76	6.26	11.83
MinAtar-median	2.07	1.56	3.33	4.95
Atari100K-mean	32.8	28.72	43.62	50.49
Atari100K-median	13.39	16.89	23.74	30.07

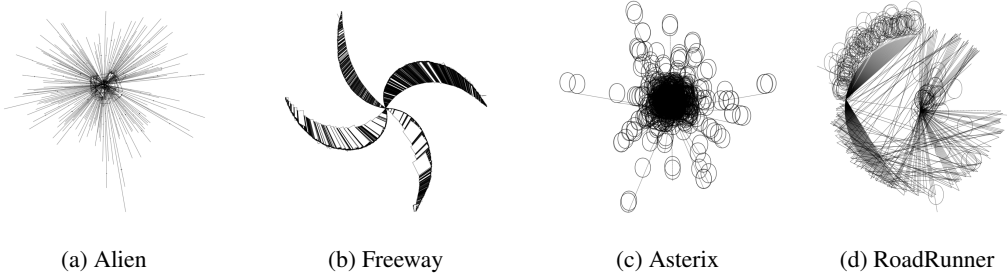


Figure 4: Transition graphs of selected Atari100K games, with data collected by a one-step DQN agent. As there are too many state nodes, we did not paint nodes directly but rather preserves edges (transitions), where circles represent self-loop transitions.

downsampling. The frame is processed into an 84 by 84 greyscale image and the observation is a stack of 4 previous frames, which leads to very sparse transition graphs.⁴ The baseline we chose for Atari100K is data-efficient Rainbow van Hasselt et al. (2019), which is a variation of Rainbow that is optimized particularly for Atari100K. Consistent with the results in MiniGrid and MinAtar, Graph Backup performs better than one-step and multi-step methods. The results here show: 1) Graph Backup is robust in terms of bringing orthogonal improvements over other DQN improvements. 2) Graph Backup works for high-dimensional, pixel-based tasks that have sparse transition graphs.

6 Analysis

Atari Transition Graphs. Here we study why Graph Backup can bring benefits to Atari games. Atari games have pixel-based observations, which have $255^{(210 \times 180 \times 3)}$ combinations if each pixel can take any value independently with other pixels. The first question is then: are there crossovers in just 100K transitions? To analyse the graph density quantitatively, we propose to measure the novel state ratio. The novel state ratio is the ratio between the amount of non-duplicated (i.e. unique) states and the amount of all states that the agent has seen. The novel state ratio will be 1 if there are no overlapping states in the transition graph, in which case Graph Backup reduces to Tree Backup. The average novel state ratio of Atari is 0.927, which means the graphs are usually quite sparse (The average novel state ratios of MiniGrid/MinAtar are 0.006/0.298 respectively). However, if we assume that duplicated states happen independently, this means that in 53% of the backup updates, there will be a crossover on the next 10 steps, which means the Graph Backup will give a different value estimate to multi-step methods more than half the time.

However, the crossovers are not distributed uniformly on the transitions graph. In order to investigate the topology of the graph, we visualize the exact graph structure of the whole transition graph. In Figure 4, we show four representative transition graphs and leave the others to Figure 7 in the Appendix. We apply *radial layouts* as proposed by Wills (1999), which scales well with the number of nodes and aligns well with the transition structure of most of the games, where the central point corresponds to the start of the game. Many transition graphs of Atari100k games show interesting crossover structures that can be leveraged by Graph Backup. For example, the transition graph of *Freeway* forms a windmill-like pattern, where each blade corresponds to a group of trajectories that have connections within the group but between groups. There are also some tasks (e.g. *Alien*) where crossovers mostly happen in the starting stage of the game.

Explaining Crossovers. By comparing the transition graphs and the pixel observations, we can provide two explanations for the existence of the trajectory crossovers in Atari games. The first factor is that there is a low number of degrees of freedom for the objects and especially for the agent avatar in many of these games. For most of the Atari games, the agent can only move on a 2D plane, which partially alleviate the curse of dimensionality since we only need two dimensions of specify the position of the agent. Imagine a large minigrid empty room task: It is difficult for a agent to sweep through the whole state space, but the crossovers can easily happen. While there are other objects

⁴Since the agent interacts with the environment every 4 frames, such preprocessing still assumes the transition to be Markovian.

moving on the screen, these are usually moving in fixed patterns which sometimes only provide one more degree of freedom: time. The agent can also interact with other objects in the game field, for example launch a projectile, allowing more branching of the transition graph. However, the learned policy will reduce the branching factor as the parameterised optimal policy is deterministic in the Q learning setup. A second important factor is that Atari games always has a fixed initial state. Although we follow prior work (Hessel et al., 2018) to add random number of no-ops after the start of the game, the initial observations the agent sees will still be quite similar, and this creates crossovers at the beginning of the episode (the centre of the plot, for example for Alien in Figure 4).

In light of these characteristics, we recommend practitioners apply Graph Backup to tasks that either (1) have few degrees of freedom, (2) have a discrete state space, or (3) are highly repetitive with minimal noise. There are many real world tasks that have similar properties, such as any 2D navigation (e.g. household cleaning robots), power management and manufacturing in assembly lines.

7 Conclusion

In this work, we motivate the introduction of a novel bootstrapped value estimation operator, Graph Backup. This backup method utilises the graph-structured nature of MDP transition data to enable counterfactual credit assignment and variance reduction. We demonstrate Graph Backup surpasses multi-step and one-step backup in MiniGrid, Minatar and Atari100K tasks.

7.1 Limitations and Future Extensions

The high level insight of Graph Backup is to treat all the transition data as a collective entity rather than independent trajectories, and exploit its (graphical) structure for sake of efficient learning. This work shows a simple implementation of this idea, by building the graph with exact state matching. While there are already a large class of tasks have crossovers, we expect in future to extend Graph Backup to cover even more challenging tasks. For example, with a learned or human-crafted discrete representation of the true state, Graph Backup might be able to tackle continuous control or tasks with partial observability. Learning a discrete representation from data has been studied in the wider deep learning community (van den Oord et al., 2017; Hu et al., 2017). In the RL context, Hafner et al. (2021b) and Kaiser et al. (2020b) use a discrete representation of the observation in their world model. Some exploration methods also require a soft matching of states (Tang et al., 2017; Bellemare et al., 2016; Ecoffet et al., 2021; Badia et al., 2020). Another way to increase the density of the graph is to create imaginary links on top of the raw graph, related to link prediction problem in knowledge graph literature. Similar approaches can potentially be applied for Graph Backup to create more crossovers, and we look forward to exploring this space. We also only utilise the transition graph for improving backup, and it's likely (as discussed in Section 2 that there are other complementary approaches that utilise the transition graph in other ways that could be combined with Graph Backup in future work.

Acknowledgements The work is supported by Amazon Alexa. We thank to Yicheng Luo and members of UCL DARK for insightful discussion.

References

- Anonymous (2022). Topological experience replay. In *Hong, Zhang-Wei and Chen, Tao and Lin, Yen-Chen and Pajarinen, Joni and Agrawal, Pulkit*. under review.
- Badia, A. P., Sprechmann, P., Vitvitskyi, A., Guo, Z. D., Piot, B., Kapturowski, S., Tieleman, O., Arjovsky, M., Pritzel, A., Bolt, A., and Blundell, C. (2020). Never give up: Learning directed exploration strategies. In *8th International Conference on Learning Representations, ICLR 2020, Addis Ababa, Ethiopia, April 26-30, 2020*. OpenReview.net.
- Bellemare, M. G., Dabney, W., and Munos, R. (2017). A distributional perspective on reinforcement learning. In Precup, D. and Teh, Y. W., editors, *Proceedings of the 34th International Conference on Machine Learning, ICML 2017, Sydney, NSW, Australia, 6-11 August 2017*, volume 70 of *Proceedings of Machine Learning Research*, pages 449–458. PMLR.

- Bellemare, M. G., Srinivasan, S., Ostrovski, G., Schaul, T., Saxton, D., and Munos, R. (2016). Unifying count-based exploration and intrinsic motivation. In Lee, D. D., Sugiyama, M., von Luxburg, U., Guyon, I., and Garnett, R., editors, *Advances in Neural Information Processing Systems 29: Annual Conference on Neural Information Processing Systems 2016, December 5-10, 2016, Barcelona, Spain*, pages 1471–1479.
- Berner, C., Brockman, G., Chan, B., Cheung, V., Debiak, P., Dennison, C., Farhi, D., Fischer, Q., Hashme, S., Hesse, C., Józefowicz, R., Gray, S., Olsson, C., Pachocki, J., Petrov, M., de Oliveira Pinto, H. P., Raiman, J., Salimans, T., Schlatter, J., Schneider, J., Sidor, S., Sutskever, I., Tang, J., Wolski, F., and Zhang, S. (2019). Dota 2 with large scale deep reinforcement learning. *CoRR*, abs/1912.06680.
- Chevalier-Boisvert, M., Willems, L., and Pal, S. (2018). Minimalistic gridworld environment for openai gym. <https://github.com/maximecb/gym-minigrid>.
- Ecoffet, A., Huizinga, J., Lehman, J., Stanley, K. O., and Clune, J. (2021). First return, then explore. *Nature*, 590(7847):580–586.
- Farquhar, G., Rocktäschel, T., Igl, M., and Whiteson, S. (2018). Treeqn and atreec: Differentiable tree-structured models for deep reinforcement learning. In *6th International Conference on Learning Representations, ICLR 2018, Vancouver, BC, Canada, April 30 - May 3, 2018, Conference Track Proceedings*. OpenReview.net.
- Fortunato, M., Azar, M. G., Piot, B., Menick, J., Hessel, M., Osband, I., Graves, A., Mnih, V., Munos, R., Hassabis, D., Pietquin, O., Blundell, C., and Legg, S. (2018). Noisy networks for exploration. In *6th International Conference on Learning Representations, ICLR 2018, Vancouver, BC, Canada, April 30 - May 3, 2018, Conference Track Proceedings*. OpenReview.net.
- Ha, D. and Schmidhuber, J. (2018). Recurrent world models facilitate policy evolution. In Bengio, S., Wallach, H. M., Larochelle, H., Grauman, K., Cesa-Bianchi, N., and Garnett, R., editors, *Advances in Neural Information Processing Systems 31: Annual Conference on Neural Information Processing Systems 2018, NeurIPS 2018, December 3-8, 2018, Montréal, Canada*, pages 2455–2467.
- Hafner, D., Lillicrap, T. P., Norouzi, M., and Ba, J. (2021a). Mastering atari with discrete world models. In *9th International Conference on Learning Representations, ICLR 2021, Virtual Event, Austria, May 3-7, 2021*. OpenReview.net.
- Hafner, D., Lillicrap, T. P., Norouzi, M., and Ba, J. (2021b). Mastering atari with discrete world models. In *9th International Conference on Learning Representations, ICLR 2021, Virtual Event, Austria, May 3-7, 2021*. OpenReview.net.
- Hernandez-Garcia, J. F. and Sutton, R. S. (2019). Understanding multi-step deep reinforcement learning: A systematic study of the DQN target. *CoRR*, abs/1901.07510.
- Hessel, M., Danihelka, I., Viola, F., Guez, A., Schmitt, S., Sifre, L., Weber, T., Silver, D., and van Hasselt, H. (2021). Muesli: Combining improvements in policy optimization. *arXiv preprint arXiv:2104.06159*.
- Hessel, M., Modayil, J., van Hasselt, H., Schaul, T., Ostrovski, G., Dabney, W., Horgan, D., Piot, B., Azar, M. G., and Silver, D. (2018). Rainbow: Combining improvements in deep reinforcement learning. In McIlraith, S. A. and Weinberger, K. Q., editors, *Proceedings of the Thirty-Second AAAI Conference on Artificial Intelligence, (AAAI-18), the 30th innovative Applications of Artificial Intelligence (IAAI-18), and the 8th AAAI Symposium on Educational Advances in Artificial Intelligence (EAAI-18), New Orleans, Louisiana, USA, February 2-7, 2018*, pages 3215–3222. AAAI Press.
- Hu, W., Miyato, T., Tokui, S., Matsumoto, E., and Sugiyama, M. (2017). Learning discrete representations via information maximizing self-augmented training. In Precup, D. and Teh, Y. W., editors, *Proceedings of the 34th International Conference on Machine Learning, ICML 2017, Sydney, NSW, Australia, 6-11 August 2017*, volume 70 of *Proceedings of Machine Learning Research*, pages 1558–1567. PMLR.

- Huber, P. J. (1992). Robust estimation of a location parameter. In *Breakthroughs in statistics*, pages 492–518. Springer.
- Kaiser, L., Babaeizadeh, M., Milos, P., Osinski, B., Campbell, R. H., Czechowski, K., Erhan, D., Finn, C., Kozakowski, P., Levine, S., Mohiuddin, A., Sepassi, R., Tucker, G., and Michalewski, H. (2020a). Model based reinforcement learning for atari. In *8th International Conference on Learning Representations, ICLR 2020, Addis Ababa, Ethiopia, April 26-30, 2020*. OpenReview.net.
- Kaiser, L., Babaeizadeh, M., Milos, P., Osinski, B., Campbell, R. H., Czechowski, K., Erhan, D., Finn, C., Kozakowski, P., Levine, S., Mohiuddin, A., Sepassi, R., Tucker, G., and Michalewski, H. (2020b). Model based reinforcement learning for atari. In *8th International Conference on Learning Representations, ICLR 2020, Addis Ababa, Ethiopia, April 26-30, 2020*. OpenReview.net.
- Mnih, V., Kavukcuoglu, K., Silver, D., Rusu, A. A., Veness, J., Bellemare, M. G., Graves, A., Riedmiller, M. A., Fidjeland, A., Ostrovski, G., Petersen, S., Beattie, C., Sadik, A., Antonoglou, I., King, H., Kumaran, D., Wierstra, D., Legg, S., and Hassabis, D. (2015). Human-level control through deep reinforcement learning. *Nat.*, 518(7540):529–533.
- Moriarty, D. E. and Miikkulainen, R. (1995). Efficient learning from delayed rewards through symbiotic evolution. In Prieditis, A. and Russell, S. J., editors, *Machine Learning, Proceedings of the Twelfth International Conference on Machine Learning, Tahoe City, California, USA, July 9-12, 1995*, pages 396–404. Morgan Kaufmann.
- Munos, R., Stepleton, T., Harutyunyan, A., and Bellemare, M. G. (2016). Safe and efficient off-policy reinforcement learning. In Lee, D. D., Sugiyama, M., von Luxburg, U., Guyon, I., and Garnett, R., editors, *Advances in Neural Information Processing Systems 29: Annual Conference on Neural Information Processing Systems 2016, December 5-10, 2016, Barcelona, Spain*, pages 1046–1054.
- Precup, D., Sutton, R. S., and Singh, S. P. (2000). Eligibility traces for off-policy policy evaluation. In Langley, P., editor, *Proceedings of the Seventeenth International Conference on Machine Learning (ICML 2000), Stanford University, Stanford, CA, USA, June 29 - July 2, 2000*, pages 759–766. Morgan Kaufmann.
- Rummery, G. A. and Niranjan, M. (1994). *On-line Q-learning using connectionist systems*, volume 37. Citeseer.
- Schaul, T., Quan, J., Antonoglou, I., and Silver, D. (2016). Prioritized experience replay. In Bengio, Y. and LeCun, Y., editors, *4th International Conference on Learning Representations, ICLR 2016, San Juan, Puerto Rico, May 2-4, 2016, Conference Track Proceedings*.
- Schrittwieser, J., Antonoglou, I., Hubert, T., Simonyan, K., Sifre, L., Schmitt, S., Guez, A., Lockhart, E., Hassabis, D., Graepel, T., et al. (2020). Mastering atari, go, chess and shogi by planning with a learned model. *Nature*, 588(7839):604–609.
- Schwarzer, M., Anand, A., Goel, R., Hjelm, R. D., Courville, A. C., and Bachman, P. (2021). Data-efficient reinforcement learning with self-predictive representations. In *9th International Conference on Learning Representations, ICLR 2021, Virtual Event, Austria, May 3-7, 2021*. OpenReview.net.
- Silver, D., Huang, A., Maddison, C. J., Guez, A., Sifre, L., van den Driessche, G., Schrittwieser, J., Antonoglou, I., Panneershelvam, V., Lanctot, M., Dieleman, S., Grawe, D., Nham, J., Kalchbrenner, N., Sutskever, I., Lillicrap, T. P., Leach, M., Kavukcuoglu, K., Graepel, T., and Hassabis, D. (2016). Mastering the game of go with deep neural networks and tree search. *Nat.*, 529(7587):484–489.
- Silver, D., Hubert, T., Schrittwieser, J., Antonoglou, I., Lai, M., Guez, A., Lanctot, M., Sifre, L., Kumaran, D., Graepel, T., et al. (2017). Mastering chess and shogi by self-play with a general reinforcement learning algorithm. *arXiv preprint arXiv:1712.01815*.
- Sutton, R. S. (1988). Learning to predict by the methods of temporal differences. *Machine learning*, 3(1):9–44.
- Sutton, R. S. and Barto, A. G. (2018). *Reinforcement Learning: An Introduction*. A Bradford Book, Cambridge, MA, USA.

- Tang, H., Houthooft, R., Foote, D., Stooke, A., Chen, X., Duan, Y., Schulman, J., Turck, F. D., and Abbeel, P. (2017). #exploration: A study of count-based exploration for deep reinforcement learning. In Guyon, I., von Luxburg, U., Bengio, S., Wallach, H. M., Fergus, R., Vishwanathan, S. V. N., and Garnett, R., editors, *Advances in Neural Information Processing Systems 30: Annual Conference on Neural Information Processing Systems 2017, December 4-9, 2017, Long Beach, CA, USA*, pages 2753–2762.
- Touati, A., Bacon, P., Precup, D., and Vincent, P. (2018). Convergent TREE BACKUP and RETRACE with function approximation. In Dy, J. G. and Krause, A., editors, *Proceedings of the 35th International Conference on Machine Learning, ICML 2018, Stockholmässan, Stockholm, Sweden, July 10-15, 2018*, volume 80 of *Proceedings of Machine Learning Research*, pages 4962–4971. PMLR.
- van den Oord, A., Vinyals, O., and Kavukcuoglu, K. (2017). Neural discrete representation learning. In Guyon, I., von Luxburg, U., Bengio, S., Wallach, H. M., Fergus, R., Vishwanathan, S. V. N., and Garnett, R., editors, *Advances in Neural Information Processing Systems 30: Annual Conference on Neural Information Processing Systems 2017, December 4-9, 2017, Long Beach, CA, USA*, pages 6306–6315.
- van Hasselt, H., Guez, A., and Silver, D. (2016). Deep reinforcement learning with double q-learning. In Schuurmans, D. and Wellman, M. P., editors, *Proceedings of the Thirtieth AAAI Conference on Artificial Intelligence, February 12-17, 2016, Phoenix, Arizona, USA*, pages 2094–2100. AAAI Press.
- van Hasselt, H., Hessel, M., and Aslanides, J. (2019). When to use parametric models in reinforcement learning? In Wallach, H. M., Larochelle, H., Beygelzimer, A., d’Alché-Buc, F., Fox, E. B., and Garnett, R., editors, *Advances in Neural Information Processing Systems 32: Annual Conference on Neural Information Processing Systems 2019, NeurIPS 2019, December 8-14, 2019, Vancouver, BC, Canada*, pages 14322–14333.
- van Hasselt, H., Madjiheurem, S., Hessel, M., Silver, D., Barreto, A., and Borsa, D. (2021). Expected eligibility traces. In *Thirty-Fifth AAAI Conference on Artificial Intelligence, AAAI 2021, Thirty-Third Conference on Innovative Applications of Artificial Intelligence, IAAI 2021, The Eleventh Symposium on Educational Advances in Artificial Intelligence, EAAI 2021, Virtual Event, February 2-9, 2021*, pages 9997–10005. AAAI Press.
- Vinyals, O., Babuschkin, I., Czarnecki, W. M., Mathieu, M., Dudzik, A., Chung, J., Choi, D. H., Powell, R., Ewalds, T., Georgiev, P., Oh, J., Horgan, D., Kroiss, M., Danihelka, I., Huang, A., Sifre, L., Cai, T., Agapiou, J. P., Jaderberg, M., Vezhnevets, A. S., Leblond, R., Pohlen, T., Dalibard, V., Budden, D., Sulsky, Y., Molloy, J., Paine, T. L., Gülcöhre, Ç., Wang, Z., Pfaff, T., Wu, Y., Ring, R., Yogatama, D., Wünsch, D., McKinney, K., Smith, O., Schaul, T., Lillicrap, T. P., Kavukcuoglu, K., Hassabis, D., Apps, C., and Silver, D. (2019). Grandmaster level in starcraft II using multi-agent reinforcement learning. *Nat.*, 575(7782):350–354.
- Wang, Z., Schaul, T., Hessel, M., van Hasselt, H., Lanctot, M., and de Freitas, N. (2016). Dueling network architectures for deep reinforcement learning. In Balcan, M. and Weinberger, K. Q., editors, *Proceedings of the 33nd International Conference on Machine Learning, ICML 2016, New York City, NY, USA, June 19-24, 2016*, volume 48 of *JMLR Workshop and Conference Proceedings*, pages 1995–2003. JMLR.org.
- Wills, G. J. (1999). Nicheworks—interactive visualization of very large graphs. *Journal of Computational and Graphical Statistics*, 8(2):190–212.
- Young, K. and Tian, T. (2019). Minatar: An atari-inspired testbed for thorough and reproducible reinforcement learning experiments. *arXiv preprint arXiv:1903.03176*.
- Zhu, G., Lin, Z., Yang, G., and Zhang, C. (2020). Episodic reinforcement learning with associative memory. In *8th International Conference on Learning Representations, ICLR 2020, Addis Ababa, Ethiopia, April 26-30, 2020*. OpenReview.net.

A Other Empirical Findings

In general, the experiments in three different settings shows Graph Backup consistently brings improvements over multi-step methods. Besides that, we also find that the improvements of n -step- Q backup over one-step backup are actually quite limited in the data-efficient setting, whereas Tree Backup performs significantly better than n -step- Q backup. This can be explained by the off-policy nature of Tree Backup, as it can bring the benefits of multi-step reward propagation without biasing the value estimation. In data-efficient setting, the flaw of n -step- Q is amplified as the learning relies more on historical rather than freshly sampled data. Interestingly, Tree Backup has not received a lot of attention in DRL community. Hernandez-Garcia and Sutton (2019) tested Tree Backup in a toy mountain car experiment which shows n -step- Q performs best among multiple multi-step methods, including Tree Backup. (Touati et al., 2018) points out the instability of Tree Backup when combined with functional approximation, both with theoretical analysis and empirically evaluation on some constructed counter-example MDPs. However, our experiments on a larger scale and more diverse set of tasks show Tree Backup has superior sample efficiency when combined with a modern DRL method.

B Pesudocode for Local Graph Expansion and Graph Backup with Rainbow Ingredients

Algorithm 1 Local Graph Expansion

Input: source state S_{source} , source action A_{source} , depth limit d , breath limit b , frequency mapping $f : \mathcal{T} \rightarrow \mathbb{N}^+$

- 1: Initialize the set containing states on the boundary of expansion $\mathcal{S}_{\text{new}} \leftarrow \{S_{\text{source}}\}$
- 2: Initialize the list of expanded state-action pairs L , denoting the largest element to be l_{\max}
- 3: **for** $i = 0$ to d **do**
- 4: Find all transitions on boundary $\mathcal{T}_{\text{new}} \leftarrow \{t | \forall t = (s, a, r, s') \in \mathcal{T}, s \in \mathcal{S}_{\text{new}}\}$
- 5: Sample b transitions from \mathcal{T}_{new} with $p(t) \propto f(t)$, getting $\mathcal{T}_{\text{pruned}} = \{t_1, t_2, \dots, t_b\}$
- 6: Append state-action pairs to list L , $\{l_{\max+1}, l_{\max+2}, \dots\} = \{(s, a) | \forall (s, a, r, s') \in \mathcal{T}_{\text{pruned}}\}$
- 7: Update boundary states $\mathcal{S}_{\text{new}} = \{s' | \forall (s, a, r, s') \in \mathcal{T}_{\text{pruned}}\}$
- 8: **end for**
- 9: **return** L

Algorithm 2 Double Distributional Graph Backup

Input: source state S_{source} , source action A_{source} , frequency mapping $f : \mathcal{T} \rightarrow \mathbb{N}^+$, list of states in the subgraph L , atoms z_0, z_1, \dots, z_{N-1} , online network $p(\cdot, \cdot | \theta)$ and target network $p(\cdot, \cdot | \theta')$

- 1: Set S_{expanded} be the set containing all the states in list L
- 2: Initialize the target values $\bar{G}_s^a = q_{\theta'}(s, a), \forall s \in S_{\text{expanded}}, a \in \mathcal{A}$
- 3: **for** (s, a) in $l_{\max}, l_{\max-1}, \dots, l_1$ **do**
- 4: $a^* = \operatorname{argmax}_a \sum_i z_i p_i(s, a | \theta)$
- 5: $m_i(s, a) = 0, \quad i \in 0, 1, \dots, N - 1$
- 6: **for** $j \in 0, 1, \dots, N - 1$ **do**
- 7: **for** $t = (s, a, r, s') \in \mathcal{T}_{s,a}$ **do**
- 8: $z'_j \leftarrow [r + \gamma z_j]_{V_{\text{MIN}}}^{V_{\text{MAX}}}$
- 9: $b_j \leftarrow (z'_j - V_{\text{MIN}}) / \Delta z$
- 10: $l \leftarrow \lfloor b_j \rfloor, u \leftarrow \lceil b_j \rceil$
- 11: $m_l(s, a) \leftarrow m_l(s, a) + \frac{f(s, a, r, s')}{c(s, a)} p_j(x_{x+1}, a^*)(u - b_j)$
- 12: $m_u(s, a) \leftarrow m_u(s, a) + \frac{f(s, a, r, s')}{c(s, a)} p_j(x_{x+1}, a^*)(b_j - l)$
- 13: **end for**
- 14: **end for**
- 15: **end for**
- 16: **return** $m_0(S_{\text{source}}, A_{\text{source}}), \dots, m_{N-1}(S_{\text{source}}, A_{\text{source}})$

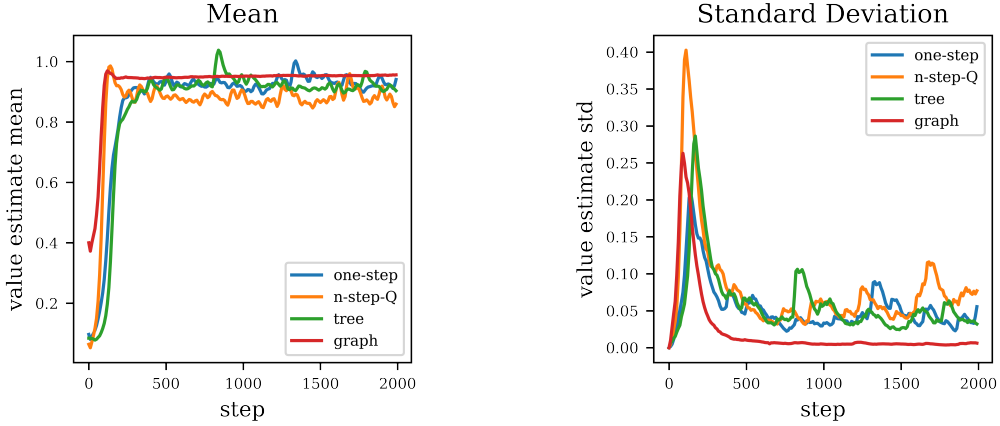


Figure 5: Mean and standard deviation of value estimate for the same state-action pairs for a fixed dataset collected in MiniGrid Empty Room. The x-axis is the number of optimization steps.

C Stable Value Estimate

Graph backup can integrate information from a subgraph, yielding a more accurate and stable value estimation. On the other hand, the nested max operators might lead to overestimation of the value. Here we try to analyse the value estimation given by different backup operators.

We collect 5000 transitions with random walks in a MiniGrid 5x5 Empty Room environment, and have the agents to learn the q^* from this static dataset. In Figure 5, we show the mean and standard deviation of latest 10 estimates of the same state-action pairs. Both mean and standard deviation are averaged over different state-action pairs. The value estimate of Graph Backup quickly stabilize after a few hundred of optimization iterations as the mean value converged and standard deviation reduce to near 0. However, all other backup methods keep giving varied estimate for the exactly same states leading to a higher standard deviation and a fluctuating mean. Notably, the MiniGrid tasks are deterministic so noise is not comes from In terms of over estimation, the graph backup do gives a slightly higher estimate at first (the little bump in the curve), however, it quickly recover to a stable value. Also, given other backup methods

D Data Graph Definition

A MDP data graph is a bipartite multi graph $(\mathcal{S}_{\text{seen}}, \mathcal{N}, \mathcal{E}_{\text{out}}, \mathcal{E}_{\text{in}})$, where $\mathcal{S}_{\text{seen}} \subseteq \mathcal{S}$ is the set of seen state nodes, $\mathcal{N} \subseteq \mathcal{S}_{\text{seen}} \times \mathcal{A}$ is the set of (state conditioned) action nodes, \mathcal{E}_{out} is a multiset of edges pointing from state nodes to action nodes and \mathcal{E}_{in} is a multiset of reward weighted edges pointing from action nodes to state nodes. A state node can point to multiple action nodes because multiple actions might be tried, and the action nodes can point to multiple state nodes because of the stochastic dynamics. When a new transition (s, a, r, s') is observed, edge $(s, (s, a))$ will be added to \mathcal{E}_{in} and $((s, a), r, s')$ will be added to \mathcal{E}_{out} . A visual example of this data graph can be seen in the Graph Backup diagram in Figure 1(b) with tried (blue) action nodes only.

Relating this data graph to Equation (6), we can see $c(s, a)$ is the number of $(s, (s, a))$ edges in \mathcal{E}_{in} and $f((s, a), r, s')$ is the number of $((s, a), r, s')$ edges \mathcal{E}_{out} .

E Details about Experiment Setup

The Graph Backup and multi-step backup both use a depth limit of 5 for MiniGrid and MinAtar, and 10 for Atari100K. The breath limit for GB-limited is 50 for MiniGrid, 20 for Minatar and 10 for Atari100K.

For MiniGrid and MinAtar, all backup methods are based on the vanilla DQN. The q network has 2 convolutions layers and 2 dense layers, and we follow the hyper-parameters of Rainbow (Hessel

et al., 2018) with target network update frequency of 8000, ϵ -greedy exploration with $\epsilon = 0.02$. The learning rate is 0.001 for MiniGrid, 0.000065 for Minatar. The discounting factor is 0.95 for MiniGrid and 0.99 for Minatar. The replay frequency is 1 for MiniGrid, and 4 for Minatar. Since we tested the algorithm in a data-efficient setting, the size of the replay buffer is set to be equal to the overall training steps.

As for Atari100K, our baselines and Graph Backup agents are based on Data-Efficient Rainbow (van Hasselt et al., 2019) with the same hyper-parameters of Schwarzer et al. (2021).

F Graph Sparsity

Across different tasks, we can see a correlation between the density of the transition graph and the improvement of Graph Backup. For MiniGrid tasks where the possible number of states are limited, the Graph Backup brings much larger improvements, whereas for MinAtar and Atari, the graph is sparse as there are multiple other objects besides the agent that can move in the game world. To analyse the graph density qualitatively, we propose the metric of the novel state ratio. The novel state ratio is the ratio between the number of non-duplicated states and the number of all states that the agent have seen. The novel state ratio will be 1 if there are no overlapping states in the transition graph, in which case Graph Backup reduces to Tree Backup. The average novel state ratio of MiniGrid/MinAtar/Atari are 0.006/0.298/0.927 respectively. The relative average improvements of Graph Backup comparing to Tree Backup are 190%/89%/17% on these three group of tasks. The graph density along, however, is not a reliable indicator to (linearly) predict how much improvement the Graph Backup can bring to a specific task. Although we know the Graph Backup will be the same as Tree Backup if the graph has no crossovers, more crossovers do not always guarantee larger performance improvement. When we investigate the normalised performance⁵ gain and the novel state ratio for each individual task we tested, the correlation is -0.29. Other factors like the structure of the graph and reward density or simply the performance upper bound can also affect the performance gain. As mentioned in Section 4.2, Graph Backup seems to bring more benefits in sparse reward tasks, which can be explained by its counterfactual reward propagation. And the structure pattern of the graph, given the same amount of crossovers, can also play a role.

G Graph Structure Visualisation

In order to investigate the topology of the graph, we visualize the exact graph structure of the whole transition graph. In Figure 4, we show four representative transition graphs and leave the others to Figure 7 in the Appendix. We apply *radial layouts* as proposed by Wills (1999), which scales well with the number of nodes and aligns well with the transition structure of most of the games. Since the common protocol for evaluating DRL agents in Atari games involves a random number of no-ops before the agent takes over the game, the initial states can vary for different episodes. To adjust for this, we create a hypothetical meta-initial state pointing to all initial states of a game. The meta-initial state is then treated as the root of the whole graph, displayed in the centre of each plot.

A lot of transition graphs of Atari100K shows interesting crossover structures that can be leveraged by Graph Backup. For example, the transition graph of *Freeway* forms a windmill-like pattern, where each blade corresponds to a group of trajectories that have connections within the group but between groups. There are also some tasks (e.g. *Alien*) where crossovers only happen during the start of the game. In such a case, the Graph Backup will not be helpful for most of the source states.

We also find some MinAtar and Atari games have self-loop states (e.g. *Asterix*), represented as circles in the graph. After further investigations, we found the existence of self-loops are because some of the state transitions in MinAtar and Atari will not make observation changes (such as periodically moving objects). This actually violates the underlining assumptions of the Graph Backup that the transitions must be Markovian, which can explain why Graph Backup is inferior to Tree Backup in some of the Tasks. On the other hand, the fact Graph Backup still outperforms multi-step methods on average suggests that Graph Backup is robust against minor violations of Markovian Assumption.

⁵The scores of MiniGrid are treated as normalised as it is. The scores of MinAtar are normalised by step 5-million-steps DQN performance reported by Young and Tian (2019)

Table 2: Full Results of all the Tasks. The agent for MiniGrid and MinAtar is based on DQN, and the agent for Atari100K is based on Data-Efficient Rainbow. The default backup operator for rainbow is n -step- Q . The values in the table for MiniGrid and Minatar are raw game scores and those for Atari100K are human-normalised scores.

	one-step	n -step- Q	tree	graph
MiniGrid-LavaCrossingS9N2-v0	0.00±0.00	0.00±0.00	0.00±0.01	0.38±0.47
MiniGrid-Empty-8x8-v0	0.69±0.35	0.11±0.07	0.96±0.00	0.96±0.00
MiniGrid-SimpleCrossingS9N2-v0	0.00±0.00	0.00±0.00	0.00±0.00	0.21±0.38
MiniGrid-KeyCorridorS3R1-v0	0.00±0.00	0.00±0.00	0.00±0.00	0.76±0.38
MiniGrid-DoorKey-6x6-v0	0.00±0.00	0.00±0.00	0.04±0.08	0.58±0.47
mean	0.14	0.02	0.2	0.58
median	0.0	0.0	0.0	0.58
Minatar-seaquest	0.53±0.25	1.12±0.40	2.68±0.87	1.77±0.64
Minatar-breakout	2.42±0.79	1.56±0.30	4.58±0.31	4.95±1.01
Minatar-asterix	2.07±1.31	2.05±0.90	3.33±1.28	2.21±1.19
Minatar-freeway	0.99±1.25	0.29±0.39	0.46±0.92	30.28±9.66
Minatar-space_invaders	9.32±1.27	13.78±4.33	20.23±2.90	19.93±3.65
mean	3.07	3.76	6.26	11.83
median	2.07	1.56	3.33	4.95
alien	5.58±0.26	9.49±2.94	7.88±0.52	6.01±1.25
amidar	6.49±0.83	8.46±2.47	5.06±0.00	5.77±2.09
assault	83.90±4.09	42.79±11.74	98.27±9.36	102.50±9.57
asterix	4.74±0.70	3.24±1.32	7.11±3.59	3.50±0.86
bank_heist	2.72±1.44	8.26±2.33	63.31±42.88	38.13±45.45
battle_zone	9.31±5.65	21.83±2.44	22.64±8.50	29.51±10.33
boxing	-98.42±90.36	-16.63±24.55	77.19±79.83	53.14±100.80
breakout	48.73±22.41	30.53±6.13	57.30±9.62	65.30±15.77
chopper_command	8.52±2.57	9.50±2.80	6.36±4.76	11.08±3.35
crazy_climber	101.27±61.26	34.85±10.15	110.68±19.87	113.45±38.87
demon_attack	24.65±15.35	3.40±1.53	24.84±8.95	23.83±12.49
freeway	53.29±38.45	61.25±50.04	35.81±50.64	64.16±46.23
frostbite	3.84±0.69	4.56±0.31	4.31±0.16	4.40±0.26
gopher	18.48±12.46	7.40±2.54	19.48±10.98	16.54±11.95
hero	17.08±15.55	22.54±2.64	31.25±7.34	30.63±2.74
jamesbond	75.72±56.84	53.47±15.43	92.52±16.12	78.80±24.20
kangaroo	29.61±9.06	143.46±90.38	76.86±62.32	141.14±84.68
krull	154.52±43.22	112.99±36.40	159.09±14.17	174.77±38.13
kung_fu_master	93.31±43.26	28.07±10.75	62.37±10.50	92.06±22.70
ms_pacman	9.71±0.85	12.94±2.94	9.11±2.38	14.60±2.49
pong	1.15±0.79	70.69±31.52	11.10±15.43	27.00±5.43
private_eye	0.11±0.00	0.11±0.00	0.11±0.00	-0.05±0.00
qbert	3.97±1.32	8.75±6.65	13.41±6.38	19.27±8.24
road_runner	167.53±141.98	42.90±21.94	116.12±115.66	164.74±130.98
seaquest	1.51±0.27	0.96±0.25	1.14±0.41	1.06±0.42
up_n_down	25.33±3.84	20.84±1.64	20.76±6.60	31.45±2.96
mean	32.8	28.72	43.62	50.49
median	13.39	16.89	23.74	30.07

H Full Experiment Results

In Table 2, we show the results of each individual task and the mean/median of the average performance in each group of tasks.

Table 3: The unnormalised scores for Atari100K. Note that taking average of these scores will lead to a evaluation metric highly weighted by games with higher score range.

	one-step	n-step-Q	tree	graph
alien	612.93±18.20	714.60±196.90	771.30±35.70	642.70±86.47
amidar	117.01±14.25	179.38±8.41	92.51±0.00	104.65±35.86
assault	658.32±21.27	422.47±37.33	733.00±48.62	754.98±49.70
asterix	603.33±58.02	497.25±18.25	799.67±297.90	500.67±71.16
bank_heist	34.27±10.61	79.50±6.20	482.00±316.83	295.97±335.86
battle_zone	5603.33±1967.76	11800.00±0.00	10243.33±2959.80	12636.67±3597.49
boxing	-11.71±10.84	0.00±0.00	9.36±9.58	6.48±12.10
breakout	15.73±6.45	10.60±0.00	18.20±2.77	20.51±4.54
chopper_command	1371.67±168.81	1103.00±0.00	1229.33±313.07	1539.67±220.49
crazy_climber	36148.17±15345.90	22990.00±0.00	38503.67±4977.60	39198.67±9737.01
demon_attack	600.42±279.20	182.00±26.40	603.90±162.70	585.48±227.10
freeway	15.78±11.38	14.96±14.96	10.60±14.99	18.99±13.69
frostbite	229.07±29.54	246.15±14.45	249.37±6.72	252.93±11.29
gopher	655.77±268.43	341.50±25.10	677.40±236.65	613.93±257.46
hero	6116.58±4635.28	7414.70±0.00	10340.43±2187.26	10154.15±817.26
jamesbond	236.33±155.64	140.75±15.75	282.33±44.13	244.75±66.25
kangaroo	935.33±270.26	1907.00±463.00	2344.67±1859.12	4262.33±2525.89
krull	3247.53±461.35	3004.35±29.75	3296.30±151.26	3463.70±407.06
kung_fu_master	21233.33±9723.05	9761.50±1777.50	14277.67±2360.11	20952.00±5102.14
ms_pacman	952.40±56.62	1015.65±14.95	912.40±158.36	1277.30±165.45
pong	-20.29±0.28	0.00±0.00	-16.78±5.45	-11.17±1.92
private_eye	100.00±0.00	0.00±0.00	100.00±0.00	-10.34±0.00
qbert	692.00±175.17	1176.75±0.00	1945.67±848.38	2724.75±1095.42
road_runner	13134.67±11122.16	4187.00±0.00	9108.00±9060.48	12916.67±10260.05
seaquest	703.13±113.31	529.20±0.00	596.27±156.14	514.53±175.51
up_n_down	3360.67±428.04	3303.50±0.00	2849.73±736.59	4043.07±330.60
mean	3744.07	2731.61	3863.86	4527.08

I All Transition Graphs

In Table 2, we visualise all the transition graphs of Atari100K.

J Mixed Graph Backup

By extending the N-Step-Q backup with the graph structure, we can get another backup target, named *mixed Graph Backup* (GB-mixed). GB-mixed only applies the max operator on the boundary nodes of the transition graph. Define $\mathcal{T}_s \stackrel{\text{def}}{=} \{(\hat{s}, \hat{a}, \hat{r}, \hat{s}') \in \mathcal{T} | \hat{s} = s\}$ and $c(s) = \sum_{T \in \mathcal{T}_s} f(T)$ similarly to before. The GB-mixed target for the state value is then:

$$\bar{G}_s = \begin{cases} \frac{1}{c(s)} \sum_{T \in \mathcal{T}_s} f(T) (\hat{r} + \gamma G_{\hat{s}'}) & \text{if } c(s) > 0 \\ \max_a q_{\theta'}(s, a) & \text{otherwise} \end{cases} \quad (7)$$

The GB-mixed target for the state-action value is then a frequency weighted average of the next state target:

$$\bar{G}_s^a = \begin{cases} \frac{1}{c(s,a)} \sum_{T \in \mathcal{T}_{s,a}} f(T) (\hat{r} + \gamma G_{\hat{s}'}) & \text{if } c(s, a) > 0 \\ q_{\theta'}(s, a) & \text{otherwise} \end{cases} \quad (8)$$

Similar to N-Step-Q backup, GB-mixed is not a strictly off-policy backup operator. The value of boundary states are estimated in an off-policy manner while the rewards of interior paths are on-policy, hence the name *mixed* Graph Backup. GB-mixed is a biased backup operator when evaluating the target policy. However, it can also be less noisy than GB-nested since there the nested max operators can propagate over-optimistic value estimation error from every step to the source state.

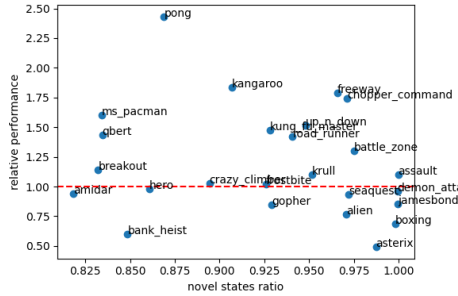
Table 4: Minatar results after 1M steps of training.

	one-step	n-step-Q	tree	graph
Minatar-seaquest	6.04±2.14	6.82±1.75	6.51±0.99	5.80±1.64
Minatar-breakout	9.83±1.70	9.28±2.94	6.56±2.18	15.03±1.50
Minatar-asterix	14.61±7.37	11.13±3.96	8.21±3.30	7.53±3.04
Minatar-freeway	39.82±26.25	5.50±5.98	19.55±27.74	39.63±26.24
Minatar-space_invaders	35.43±6.87	24.58±2.86	35.83±6.10	42.68±6.32
mean	21.14	11.46	15.33	22.13
median	14.61	9.28	8.21	15.03

K Graph Density of Atari100K

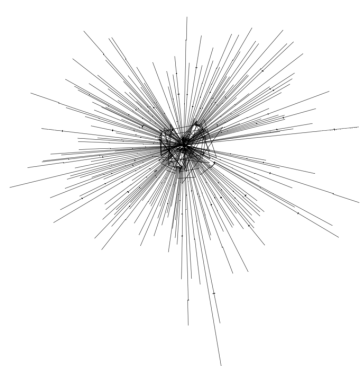
We also explore the role of graph density in the same set of tasks. In Figure 6, we show the correlation between relative performance and novel state ratio, where each point represents a task in Atari100K. The relative performance is the human normalised score of GB-nested divided by that of tree backup. It indicates how much benefits the agent can get from leveraging the graph structure. There is a negative correlation of -0.22 between novel states ratio and relative performance. Although the correlation is weaker than the case of cross-group comparison, the graph density can still affect the effectiveness of Graph Backup.

Figure 6: Relative performance and novel state ratio

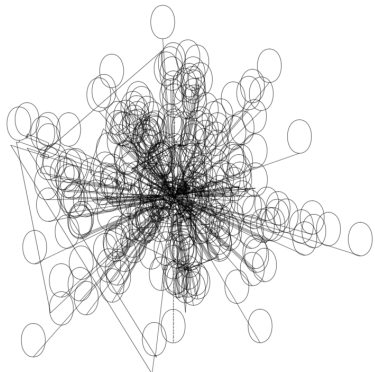


L MinAtar 1M

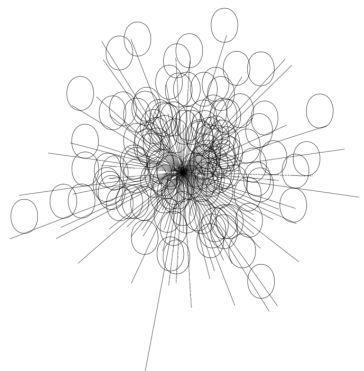
Table 4 shows the performance of different methods after 1M steps of training. Both one-step and Graph Backup achieves the means scores close to the DQN asymptotic performance reported by Young and Tian (2019). This shows that even with more training data, Graph Backup is able to converge to the same level of performance as one-step backup. Surprisingly, though, the n -step- Q backup and Tree Backup both perform worse than one-step backup with more data. This can be explained by the innate problems of n -step- Q and nested max operators. Strictly speaking, n -step- Q is not an off-policy backup operator because it always uses online reward sequences for the estimation of its value, which can counter its advantages in longer reward propagation. This can be especially true for Minatar because its framerate is much lower than vanilla Atari and longer reward propagation may not be as important. For Tree Backup and Graph Backup, the nested max operator may cause an overestimation of values. We leave methods that address this problem for future work. With the over-estimation dealt with properly, Graph Backup may show even stronger performance in an asymptotic setting.



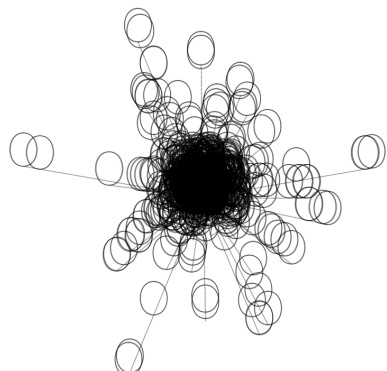
(a) Alien



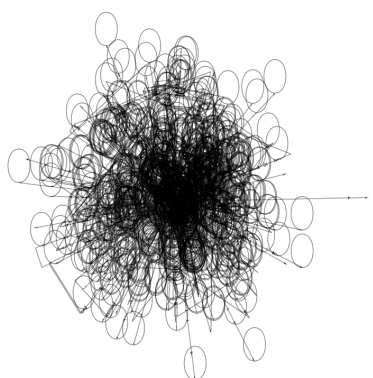
(b) Amidar



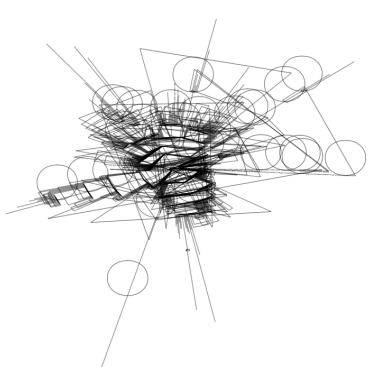
(c) Assault



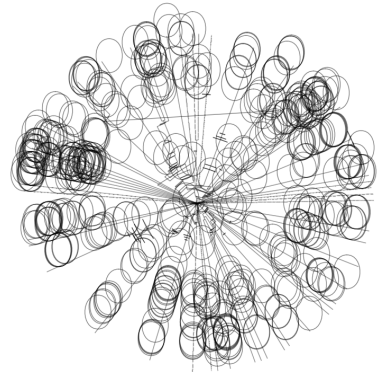
(d) Asterix



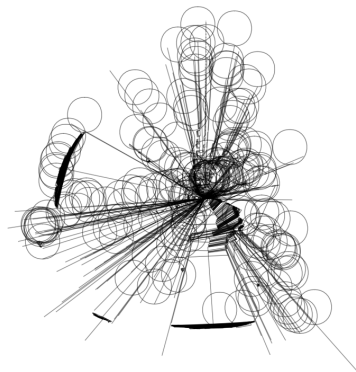
(e) Bank Heist



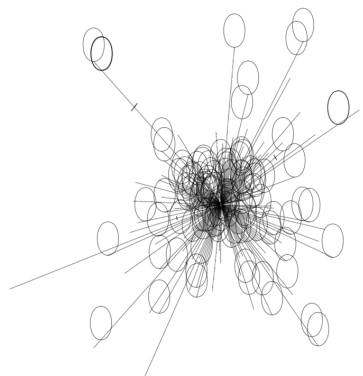
(f) Battle Zone



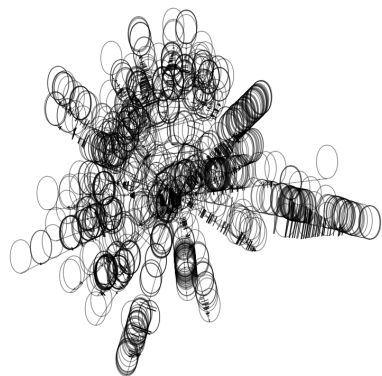
(g) Boxing



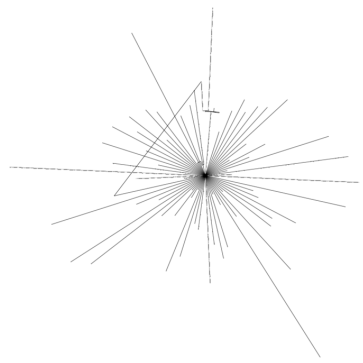
(h) Breakout



(i) Chopper Command



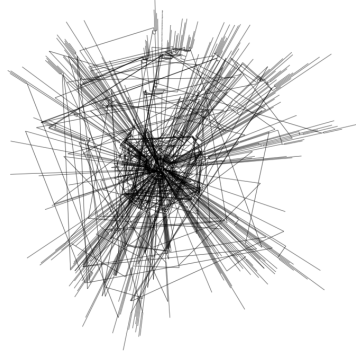
(j) Crazy Climber



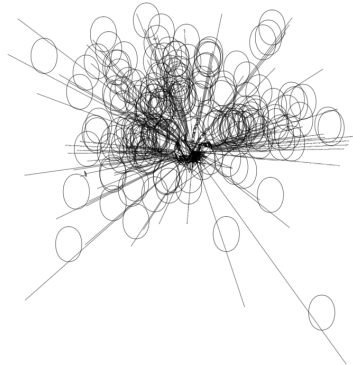
(k) Demon Attack



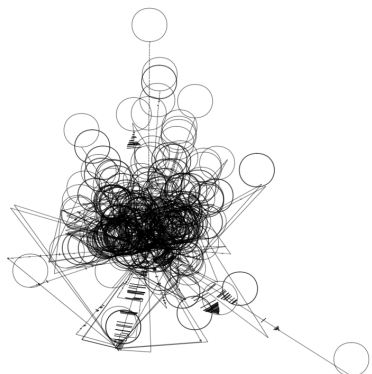
(l) Freeway



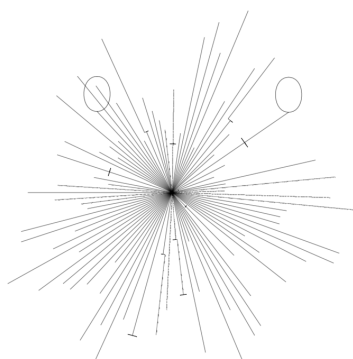
(m) Frostbite



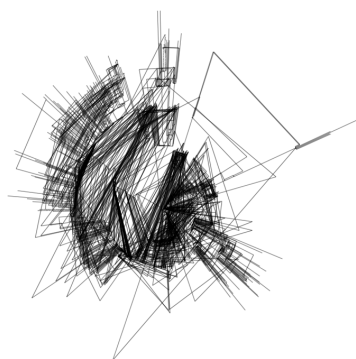
(n) Gopher



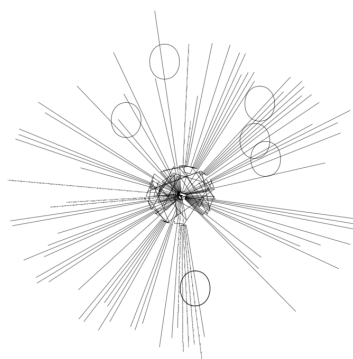
(o) Hero



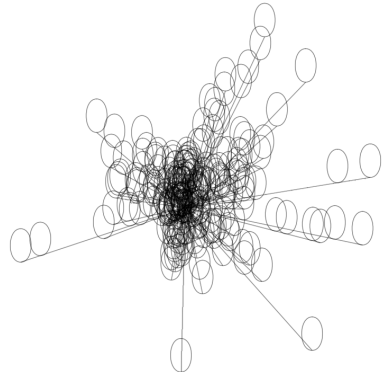
(p) Jamesbond



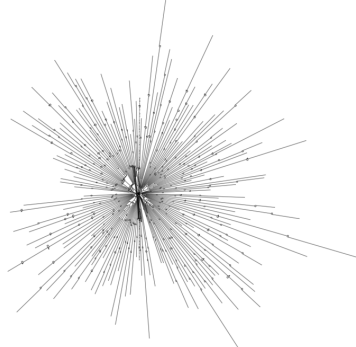
(q) Kangaroo



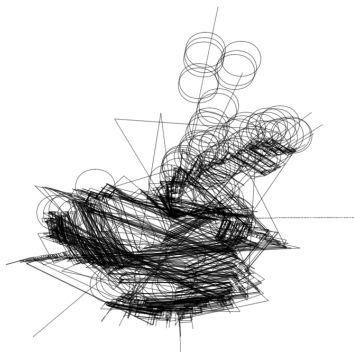
(r) Krull



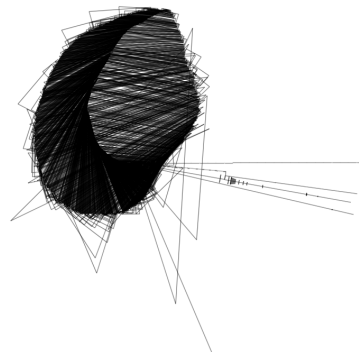
(s) Kung Fu Master



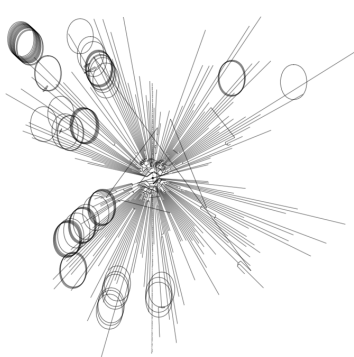
(t) Ms Pacman



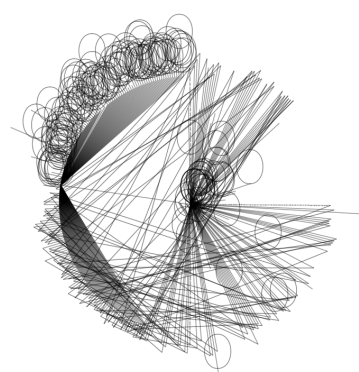
(u) Pong



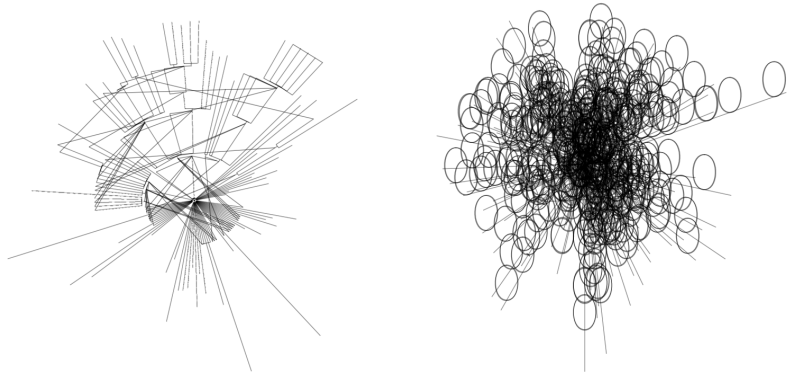
(v) Private Eye



(w) Qbert



(x) Road Runner



(y) Seaquest

(z) Up N Down

Figure 7: All Transition Graphs of Atari100K